Journal of Computational Acoustics,

SUBSPACE APPROACH TO INVERSION BY GENETIC ALGORITHMS INVOLVING MULTIPLE FREQUENCIES

PURNIMA RATILAL
DSO National Laboratories
20, Science Park Drive, Singapore 118230

PETER GERSTOFT
Marine Physical Laboratory, Scripps Institute of Oceanography
University of California, San Diego, CA 92093-0701

JOO THIAM GOH
DSO National Laboratories
20, Science Park Drive, Singapore 118230

Received (to be inserted
Revised by Publisher)

Based on waveguide physics, a subspace inversion approach is proposed. It is observed that the ability to estimate a given parameter depends on its sensitivity to the acoustic wave-field, and this sensitivity depends on frequency. At low frequencies it is mainly the bottom parameters that are most sensitive and at high frequencies the geometric parameters are the most sensitive. Thus, the parameter vector to be determined is split into two subspaces, and only part of the data that is most influenced by the parameters in each subspace is used. The data sets from the Geoacoustic Inversion Workshop (June 1997) are inverted to demonstrate the approach. In each subspace Genetic Algorithms are used for the optimization, it provides flexibility to search over a wide range of parameters and also helps in selecting data sets to be used in the inversion. During optimization, the responses from many environmental parameter sets are computed in order to estimate the *a posteriori* probabilities of the model parameters. Thus the uniqueness and uncertainty of the model parameters are assessed. Using data from several frequencies to estimate a smaller subspace of parameters iteratively provides stability and greater accuracy in the estimated parameters.

1. Introduction

Inversion by matched field processing (MFP) can be cast as a non-linear optimization problem that uses global search methods like simulated annealing[1,2] and genetic algorithms[3,4] to search over the space of likely values of the unknown parameters. The ease of inversion by MFP depends on the number of parameters to be optimized[5,6]. In general, the complexity of the problem increases with the number of unknown parameters. This is due to the presence of many local minima in the multi-dimensional parameter space which obscure the search for the global minimum. Here, it will be shown that it is possible to simplify the inversion by taking into account the physical principles of interaction of the acoustic wave-field with the environment. We were able to reduce the inversion into a number of problems with a smaller subset of parameters to optimize in each case. This greatly improved the efficiency of the optimization as the search algorithm had a smaller subspace of parameter values to search through for the global minimum in each of the reduced problem.

Following this introduction, our approach to performing the inversion by matched field processing is described. All our inversions to estimate the parameters of the various Benchmark problems were performed using the SAGA inversion code[7]. Our use of waveguide physics to reduce the dimensionality of the search space is outlined in Sec. 3. Solutions to the Benchmark problems are described and compared to the true parameter values in Sec. 4.

2. Matched Field Inversion

2.1. *Objective function*

As usual we minimize an objective function $\phi(\mathbf{m})$ for finding the most likely set of environmental parameters $\mathbf{m}$. The objective function is the incoherent sum of the Bartlett power for each frequency $l = 1 \ldots N_{\text{freq}}$. As the data contain no noise, both the observed $\mathbf{p}_l$ and computed data $\mathbf{q}_l(\mathbf{m})$ are based on pressure vectors over the array of sensors,

$$\phi = 1 - \frac{1}{N_{\text{freq}}} \sum_{l=1}^{N_{\text{freq}}} \frac{|\mathbf{p}_l^\dagger \mathbf{q}_l(\mathbf{m})|^2}{|\mathbf{p}_l|^2 |\mathbf{q}_l(\mathbf{m})|^2} , \tag{2.1}$$

where † is the complex transpose. The calculated replica is computed using the OASES wavenumber integration code[8,9] as the forward model.

2.2. *Genetic algorithms*

The global search method used for the optimization is genetic algorithms (GA). The basic principle of GA is simple: From all possible parameter vectors, an initial population of q members is randomly selected. The "fitness" of each member is computed on the basis of the value of the objective function. Based on the fitness of the members a set of "parents" are selected and through a randomization process a set of "children" is produced. These children replace the least fit of the original population and the process iterates to evolve into an overall more fit population. A detailed description of genetic algorithms and their application to parameter estimation is given in Gerstoft[3].

The GA search parameters were selected as follows. The population size was set to 64, the reproduction size was 0.5, the crossover probability was 0.8 and the mutation probability was 0.05. The number of iterations was 1000 for each of the 10 independent populations specified. Hence a total of 10^4 forward models were performed for each selected frequency in the optimization. For each unknown parameter to be estimated, its search space was quantized into 128 increments.

2.3. *Subspace inversion*

In a subspace approach to inversion, see e.g. [10,11], the total parameter vector $\mathbf{m}$ is divided into a number of subsets of parameters denoted by A, B, C,... etc.

$$\mathbf{m} = [\mathbf{m}_A^{\mathrm{T}}, \mathbf{m}_B^{\mathrm{T}}, \mathbf{m}_C^{\mathrm{T}}, \ldots]^{\mathrm{T}} \quad , \tag{2.2}$$

where $^{\mathrm{T}}$ is the transpose. The number of subsets and the dimensionality of each subset is problem dependent. In a subspace approach, the parameters in each subset are optimized independently. The advantage of a subspace approach is that the possible search space becomes smaller in each iteration, and it is thus easier to retrieve the relevant parameters.

For a given data set and environmental model, a model covariance matrix can be introduced

$$\mathbf{C}_{\mathbf{m}} = \mathsf{E}[(\mathbf{m} - \bar{\mathbf{m}})(\mathbf{m} - \bar{\mathbf{m}})^{\mathrm{T}}] = \begin{pmatrix} \mathbf{C}_{AA} & \mathbf{C}_{AB} & \mathbf{C}_{AC} & \\ \mathbf{C}_{BA} & \mathbf{C}_{BB} & \mathbf{C}_{BC} & \\ \mathbf{C}_{CA} & \mathbf{C}_{CB} & \mathbf{C}_{CC} & \\ & & & \ddots \end{pmatrix} . \tag{2.3}$$

For a subspace method to work well it is required that the off diagonal covariance matrices be neglected relative to the diagonal matrices. Previously, we attempted to use a subspace approach by inverting for each parameter type (sound speed, attenuation, density) separately. However, this did not work and it is expected to be due to the large correlation between different parameter types. In the present approach, the number of subspaces and the ordering of parameters in subspaces is determined based on the observed data such that the off diagonal covariance matrices are small.

2.4. *Convergence*

Three indicators are used to determine the quality of the estimate. Due to the non-uniqueness of the inversion it is not guaranteed that *the* correct solution is found even when all the three criteria are satisfied.

a) Value of objective function. For a good match the objective function should approach a certain value. In particular, for the present inversion, where the parameterization is known *a priori*, it is known that $\phi \approx 0$ indicates a good match.

b) Plotting of the data and replica with the best match. A visual comparison of the data and replica can often identify problems in the inversion. Often the same data are used when comparing the match; but also data that have not been used in the inversion could be used.

c) A posteriori distributions. The purpose of the inversion is to determine a set of parameters and thus it is important to have an indication of how well each parameter has been determined. Based on the obtained samples during the inversion, statistics of the convergence for each parameter are computed. Using a Bayesian framework this can be interpreted as a Monte Carlo integration of the likelihood function[12]. However, often the likelihood function is not available and then a practical weighting of the objective function is performed to give an estimate of the *a posteriori* distributions[3,13]. Due to this ad hoc weighting, the *a posteriori* probability should be interpreted with care. The relative importance of the parameters in the same inversion is precise, but the interpretation and comparison of inversion results based on different data or approaches should be carried out with care.

3. Inversion Strategy

3.1. *Selection of Data as Observation*

The data set[14] provided as observation in each of the test cases is extensive. It covers over 200 frequencies from 25 to 500 Hz at 5 ranges from 1 to 5 km for an array of 100 receivers. Our choice of propagation code for the forward modelling is limited to what is available in the current version of SAGA, which includes the normal mode code SNAP[15], the full wavenumber integration code OASES[8,9] and broadband normal mode code ORCA[16,17]. Since OASES is also an appropriate model for the elastic problem EL, we decided to use OASES as the forward model to compute the replica acoustic fields.

A major constraint in matched field processing is computational time. Being a full-wave model, OASES is computationally more intensive than many other acoustic propagation codes based on normal mode theory. Since OASES computes the replicas at each range by stepping out in range, data at longer ranges would require more computational time. As thousands of replica acoustic fields are computed in each case, it is essential to limit the computation to small ranges. In all the test cases that we worked on, data at the closest range of 1 km were used in the objective function. Moreover, some of the unknown parameters were most sensitive to data at this range compared to any of the other ranges provided.

3.2. *Interaction of Wavefields with the Environment*

The interaction of the acoustic wave-field with the environment depends much upon its frequency. The CAL environment from the Inversion Workshop is shown in Fig. 1. The sound speed profile in the water column is downward refracting. This enhances the interaction of acoustic wave-fields with the sediment and bottom. There is a positive sound speed gradient in the sediment. The range vs depth transmission loss contour for acoustic wave-fields of frequencies 25 and 199 Hz were computed by OASES and is illustrated in Fig. 2. With regard to interaction of the acoustic wave-field with the sediment and bottom, it is evident that low frequency wave-fields propagate substantially through the sediment and bottom. High frequency wave-fields on the other hand have negligible penetration into the sediment and bottom due to high attenuation. This implies that high frequency data would be insensitive to the properties of the bottom and deeper layers of the sediment. It is the properties of the sediment close to the water-sediment interface that are important for high frequencies. Figure 3a shows the Bartlett[4] power vs bottom sound speed for the data at 1 km range from the CAL environment at the two frequencies of 25 and 199 Hz. We see that the Bartlett power variation is almost negligible at the higher frequency due to its insensitivity to the bottom sound speed.

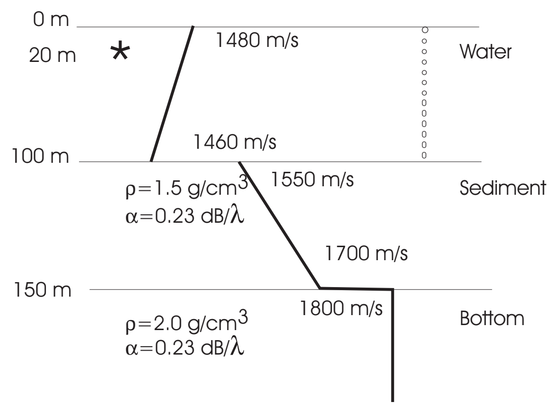

Figure 1: The CAL environment from the Inversion Workshop.

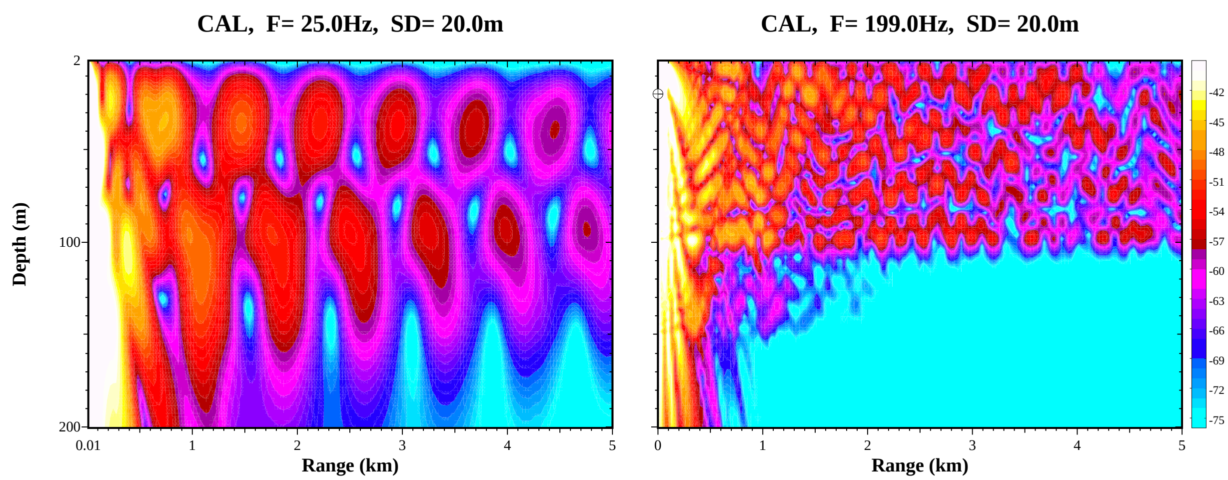

Figure 2: Case CAL: Transmission loss contours for a source depth of 20 m

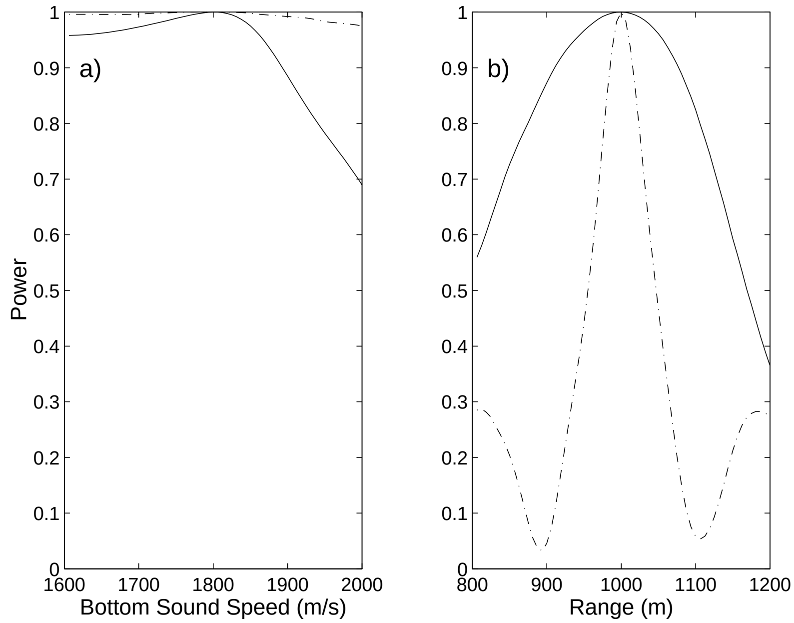

Figure 3: Case CAL: The variation in Bartlett power vs (a) bottom sound speed and (b) range using an array of 100 receivers. The frequencies are 25 Hz (solid line) and 199 Hz (dashed-dotted line). The observed data are at a range of 1 km.

From Fig. 2, it is also apparent that the variation of propagation loss with range and depth is greater at the higher frequencies. The Bartlett power variation with range for the same set of data at the two frequencies of 25 and 199 Hz is shown in Fig. 3b. The higher frequency is more sensitive to the variation in the source range.

We can conclude that wave-fields of varying frequencies have differing sensitivities to the environment and geometric parameters. In inversion problems with unknowns in both the source position and the sea bottom properties, it is essential to use a combination of both high and low frequency data as observation in the objective function. High frequencies allow estimation of the source position with greater accuracy while the lower frequencies provide reliable estimates of the sea bottom parameters.

3.3. ***Subspace Approach to Inversion***

We make use of the varying sensitivities of the wave-fields at various frequencies to reduce the inversion problem into a sequence of smaller inversions with fewer unknowns to estimate at each stage.

The parameters to be estimated in the Benchmark problems were broadly separated into those that are sensitive to high and low frequency wave-fields. An inversion sequence was adopted that used the high and low frequencies in separate runs to estimate a smaller subset of parameters in an iterative manner until a good match was obtained with the observed data. Figure 4 illustrates the iterative-subspace strategy that we employed.

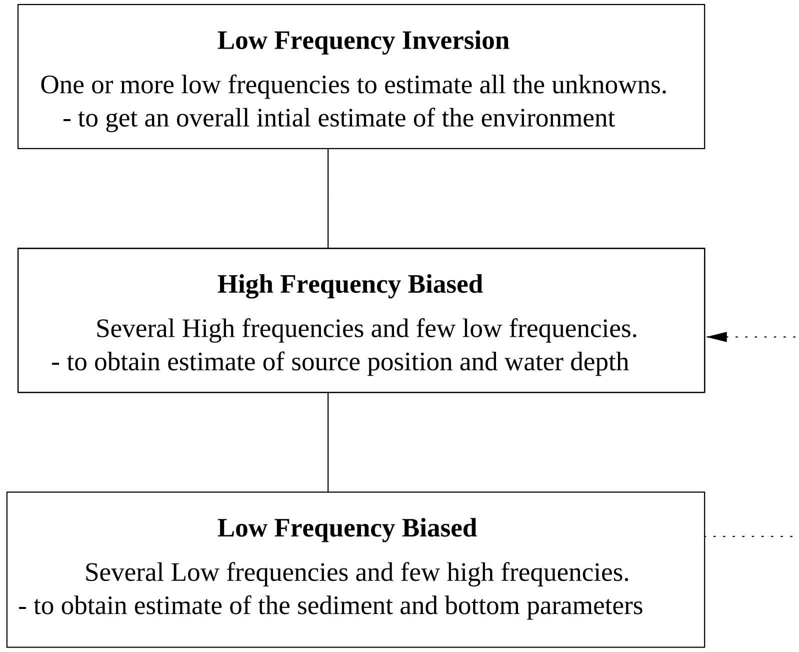

Figure 4: Scheme to implement the iterative-subspace approach to inversion which uses multiple frequencies in separate inversion runs. A smaller subset of parameters are estimated in each run.

We start off the iteration using low frequency data in the inversion to estimate all the unknowns. The main objective here is to have an overall feel for the environment and to obtain approximate estimates of the sediment and bottom parameters. The next step is a high frequency biased run to estimate the source position and water depth. Since the higher frequencies do not sample much of the bottom, the estimates of the bottom properties now are not expected to change much from those derived from the first stage of the iteration. Having estimated the source position and the water depth, we now invert for the properties of the sediment and bottom with a low frequency biased run. Here we use several low frequencies to probe the sediment and bottom. As shown in Sec. 3.2, the low frequencies are less sensitive to variations in the source range and depth. Therefore those geometric parameters estimated in the high frequency biased stage are not modified much. At this stage, we compare the fitness that we have achieved between the observed data and the predicted acoustic field from the inverted environment. If a good match is obtained (see Sec. 2.4) for the acoustic field over the frequency interval from 25 to 500 Hz, we stop the iteration. Otherwise, we repeat the high and low frequency biased steps in the inversion strategy. This loop continues till a good match is obtained.

4. Solution of the Test Cases

We worked on the following Benchmark cases from the Workshop; SD, WA and EL. SD and WA use the same parameterization of the environment as in the CAL case (see Fig. 1). In the SD case, there were 6 unknown parameters: sediment thickness, sediment density, top and bottom sediment sound speeds, bottom density and sound speed. For the case WA, there were 9 unknown parameters. In addition to the ones for the SD case, the source depth and range and the water depth were not known. For both SD and WA, data for three realizations of the environment were provided. These are denoted by A, B and C. The three environments of test case WA were estimated using the subspace approach to inversion. One inversion loop was used for environment B and multiple loops for environments A and C. The subspace method of inversion will be illustrated in the Sec. 4.1 for case WA, realization B. For SD and EL, since the source position and water depth are known, we have used a single run at low frequencies to estimate all the unknowns parameters. It is possible to improve the estimates obtained for SD by using the subspace approach. This will be elaborated in Sec. 4.2.

4.1. *WA, unknown source position and environment*

For the test case WA, there were nine unknown parameters which include the source position, water depth, sediment and bottom properties. The parameters for environment B were estimated following the iterative scheme that implements the subspace approach to inversion. As mentioned previously, we started the inversion by using data at several low frequencies to obtain approximate estimates of the nine unknown parameters. Next, the estimates for the sediment and bottom were fixed at the deduced values. For the high frequency inversion, we used data at 199 Hz only. The parameters that influence high frequency propagation were optimized. They are the source position, water depth, compressional speed and density of the sea floor. Figure 5 shows the marginal probability density distribution for the various parameters. The peak of the distribution for the source range and depth and the water depth coincides with the true parameter values indicating a successful inversion. The estimate for the speed at the top of the sediment is also close to the true value. The distribution for the sediment density, however, is scattered. Figure 6a and 6b show the Bartlett power plots for the speed at the top of the sediment and the sediment density respectively. At 199 Hz, the sediment speed is a more sensitive parameter than the sediment density as it affects the acoustic field more significantly. Therefore the sediment speed at the surface can be estimated more precisely.

With the source position and water depth accurately known, we invert for the remaining parameters using a low frequency biased run with data at 25, 35 and 50 Hz. The surficial sediment properties are included as variables here as any error in the surface sediment sound speed affects the estimation of the sound speed deeper in the sediment and in the bottom.

Figure 7 shows the marginal probability density distribution for the sediment and bottom properties. The estimate for the sediment speed at the top of the sediment now coincides with the true value. The estimates for the sediment thickness and the speed at the bottom of the sediment are slightly off the true values. Figure 8 shows the ambiguity surface, at 25 and 199 Hz, for the sediment thickness and speed at the bottom of the sediment. There is a band of values for the sediment speed and thickness for the environment that leads to

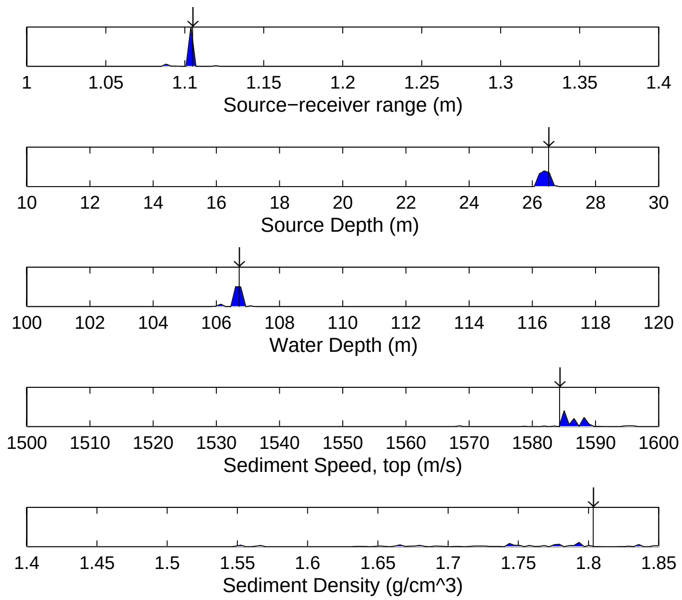

Figure 5: Case WAB: Marginal probability density distribution for the high frequency biased run. The solid line indicated by the arrow are the true values of these parameters.

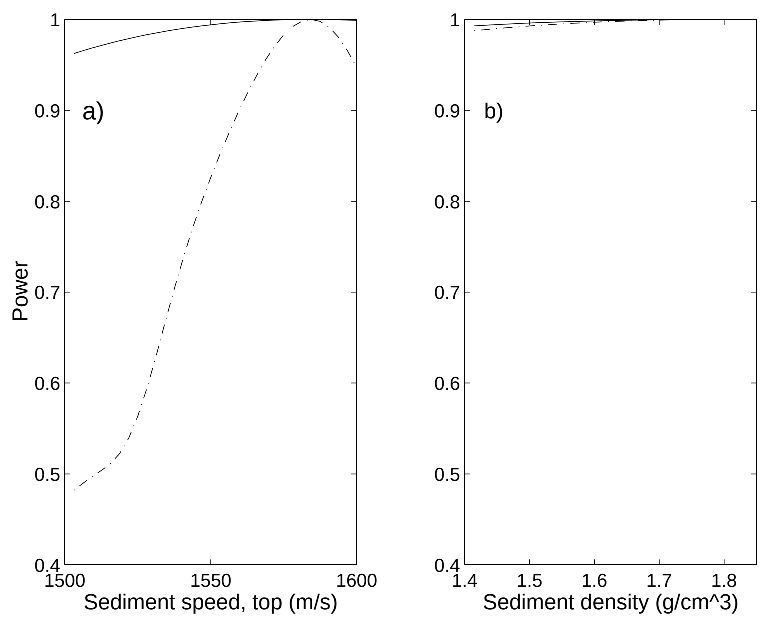

Figure 6: Case WAB: Bartlett power vs (a) sound speed at the top of the sediment and (b) sediment density for the two frequencies, 25 Hz (solid line) and 199 Hz (dashed line).

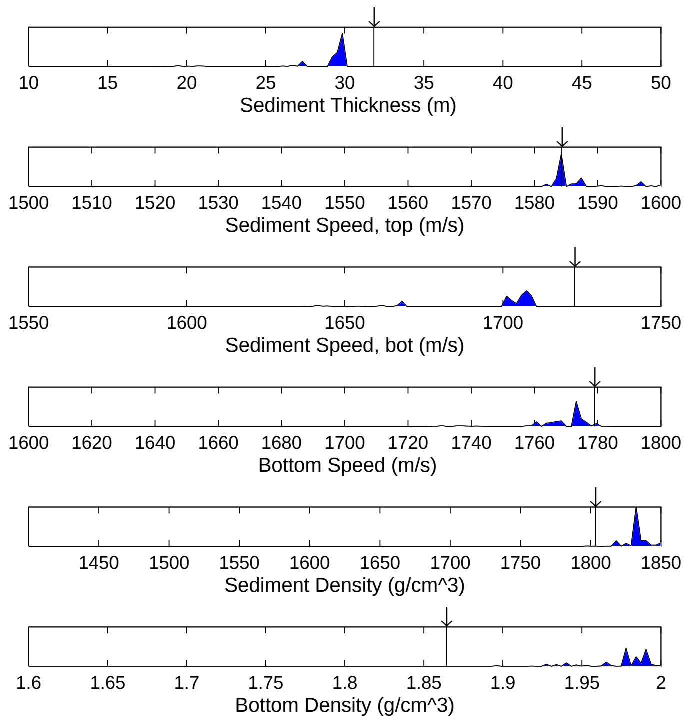

Figure 7: Case WAB: Marginal probability density distribution for the parameters affected by low frequencies. These results are for the low frequency biased run.

pressure fields with strong correlation to the observed data. This suggests that perhaps the sound speed gradient in the sediment is a more relevant parameter to invert for than the precise depth and sound speed values.

Figure 9 shows the match in the magnitude of the acoustic pressure from the inverted environment with the actual pressure field of WAB. The match obtained is good even at the higher frequencies of 300 and 500 Hz which were not used in the inversion. For the data used in the inversion, the objective function value ϕ, obtained was of the order of 10^{-3} which is very small (see Sec. 2.4a).

The iterative-subspace inversion strategy employed here is a simple extension of a similar scheme used by Siedenburg et. al. In the Workshop problems, the presence of a gradient in the sediment layer suggests that a low frequency probe (25 Hz) be used first, followed by an inversion at 199 Hz to obtain the sediment properties. In Siedenburg et. al.[6], the lack of a gradient in the sediment allows a high frequency inversion to be done first to obtain surficial sediment properties. This is then followed by a low frequency inversion to derive the bottom properties.

4.2. *Comparison between Subspace Approach and Global Inversion*

For problem SD, the geometric parameters and water depth are known. The objective is

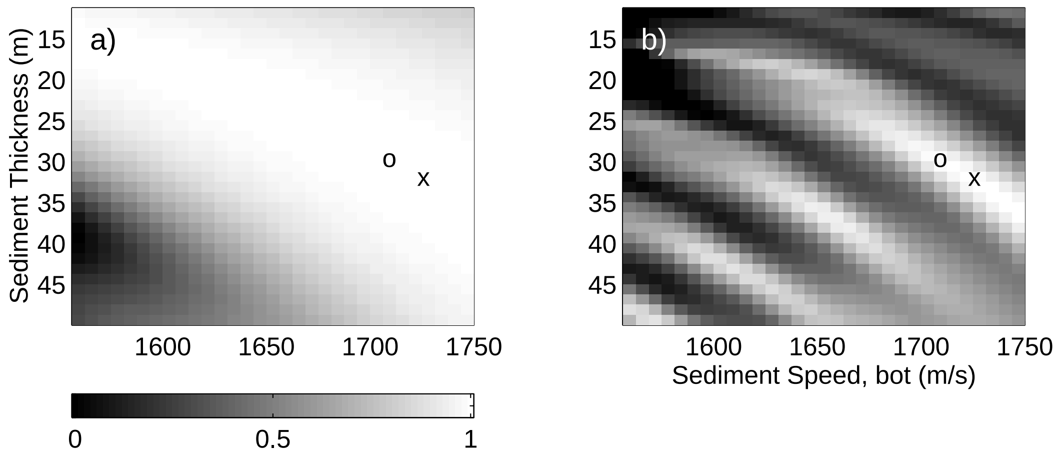

Figure 8: Case WAB: Ambiguity surface for the sound speed at the bottom of the sediment and the sediment thickness for pressure fields at (a) 25 Hz and (b) 199 Hz. The true parameter values are marked by a $\times$ and the parameter estimates from the iterative-subspace inversion approach are marked by $\circ$. Both the estimated and true parameter values lie in the high correlation band.

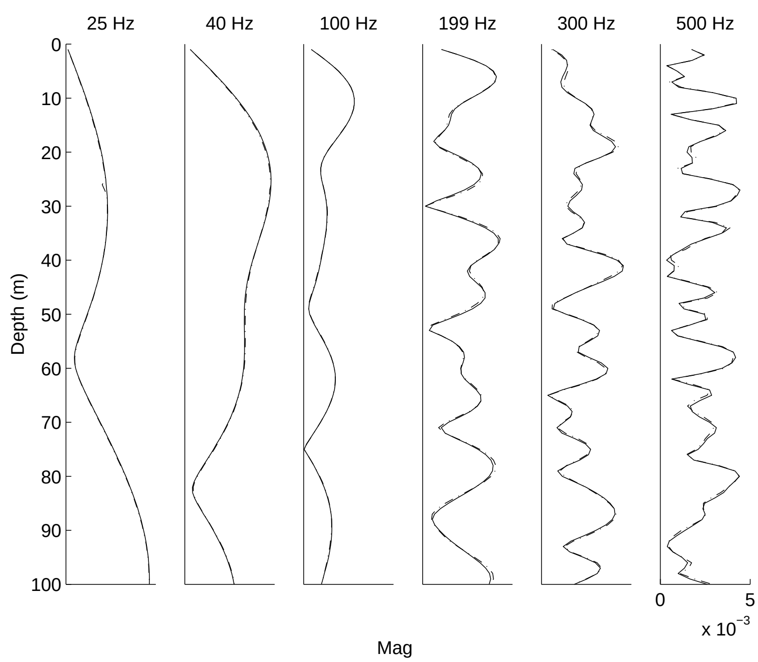

Figure 9: Case WAB: Comparison of the acoustic pressure field (magnitude) from the test data (solid line) and that from the environment obtained from inversion (dashed line) at various frequencies.

Parameter		True Value	Estimated Subspace	Estimated Global	nor. sd. Subspace	nor. sd. Global
Sediment Thickness	(m)	22.4678	22.5	19.6	0.011	0.03
Sediment Speed, top	(m/s)	1565.12	1565.4	1572.1	0.0005	0.03
Sediment Speed, bot	(m/s)	1743.14	1742.9	1708.6	0.02	0.05
Sediment layer Density	(g/cm^3)	1.75528	1.755	1.667	0.011	0.10
Basement layer Speed	(m/s)	1757.69	1758.6	1758.2	0.004	0.03
Basement layer Density	(g/cm^3)	1.83349	1.840	1.616	0.08	0.03
Fitness			4×10^{-5}	10^{-2}		

Table 1: Case SDA: Mean values of the environment properties estimated using the subspace and global inversion approaches. The associated standard deviation of each estimate by the two approaches have been normalized by the search interval. Fitness refers to the objective function value, ϕ that has been achieved.

to estimate the properties of the sediment and bottom. We employed global inversion using data at several low and intermediate frequencies to estimate all six parameters for the three environments of SD. Good matches of the predicted acoustic field to the data were obtained for environments SDB and SDC. However, in the case of SDA, the acoustic fields from the forward model using the inverted environments showed a poor match to the data. We tried to improve on the estimates for the environment SDA using the iterative inversion scheme based on the subspace approach. The high and low frequency data were used separately to estimate a smaller subset of parameters at each instance. The surficial sediment properties were estimated in the high frequency runs. The sediment thickness, speed at the sediment bottom, and the bottom properties were estimated in the low frequency biased run. Table 1 compares the estimates obtained from global inversion and iterative-subspace inversion with the true values for each parameter. The estimates are obtained from the mean of the *a posteriori* distribution[13] for each parameter. Data at the same number of frequencies were used in the global and iterative-subspace inversions, namely, 25, 35, 50, 100 and 199 Hz.

We note that the parameter estimates obtained using the iterative-subspace inversion scheme are in good agreement with the true values. However, the estimates using the global inversion do not perform as well. This is somewhat counter-intuitive since global inversion uses all the information from both high and low frequencies at the same time. We believe the poor solutions to be attributed to insufficient sampling of the parameter space. Due to practical constraints on computational time, each inversion was restricted to only 10,000 forward model runs. However, with a 128 point discretization of the search interval for each parameter, we have a total of 128^6 model vectors in a global inversion run. Thus only a small fraction of the model vectors are tested. In addition, it is also likely that in the global inversion runs, due to the complexity of the objective function surface, a 128 point sampling of the search interval may be insufficient and that the optimization strategy actually gets trapped in a local minima. On the other hand, if a more exhaustive search is performed, it is probable that the estimates from the global inversion can be improved. This however would require too much CPU time for the inversion.

4.3. *EL, Elastic Problem*

For environments with shear in the sediment and bottom, the effect of this shear on acoustic

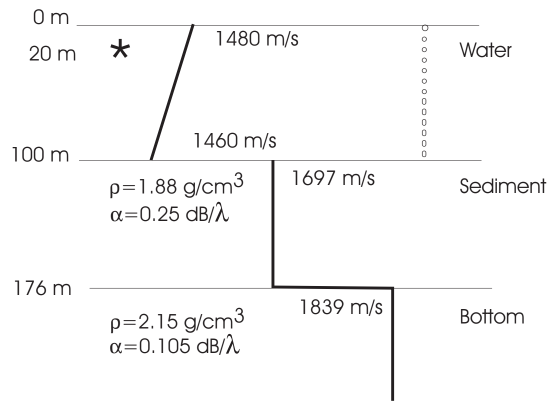

Figure 10: The EL environment, realization B from the Inversion Workshop.

propagation depends not only on the magnitude of the shear speeds in the sediment and bottom, but also on the proximity of the source to the water-sediment interface. For environment ELB (see Fig. 10), the transmission loss versus range for a receiver at a depth of 99 m and a source at depths of 20 and 99 m are shown in Figures 11a and 11b respectively. We note that when the source is close to the sediment, the effects of shear are more apparent, particularly at ranges close to the source. When the source is at 20 m depth, it is too far from the sediment to excite shear waves. Consequently, even though the sediment and bottom may support shear, the effects of shear become negligible with regard to the wave-field in the water column.

Figure 12 shows the integrand plot for a receiver at a depth of 99 m in environment ELB at a source frequency of 25 Hz. We note that to compute the field for a source at 99 m, the wavenumber integration must be carried out to larger wavenumbers than that for a source at 20 m. For the expected shear speeds in problem ELB, we expect to compute the replica acoustic fields by integrating out to wavenumbers of at least 1.5/m, corresponding to a shear speed of about 100 m/s to include the shear wave. However, from Figure 12, we note that with the source at 20 m depth, we need only integrate out to less than 0.38/m for each frequency which corresponds to a larger horizontal wave speed. We will not obtain the shear wave, but the shear sound speed will increase the attenuation of the P-waves and thus they will have an effect on the propagation[18]. Therefore it is still possible to obtain estimates of the shear wave speed. However, if also the P-wave attenuation in the sediment was unknown then it is questionable if it is possible to determine the shear sound speed.

A comparison of the inversion times with 10,000 forward model runs indicate that the computation time is reduced from 6 to 2 hours when integrating only out to wavenumbers of 0.38/m. Table 2 shows the excellent agreement between the estimated parameters and the true values. Here, a better understanding of the physics has resulted in cost savings in the computation time for the inversions.

4.4. *Summary of Solutions*

Our estimate of the parameters for the other realizations of environments SD, WA and EL are provided in Tables 3 to 5. Our approach to solving these test cases uses either iterative-subspace inversion or global inversion. The precise method used is specified in each case.

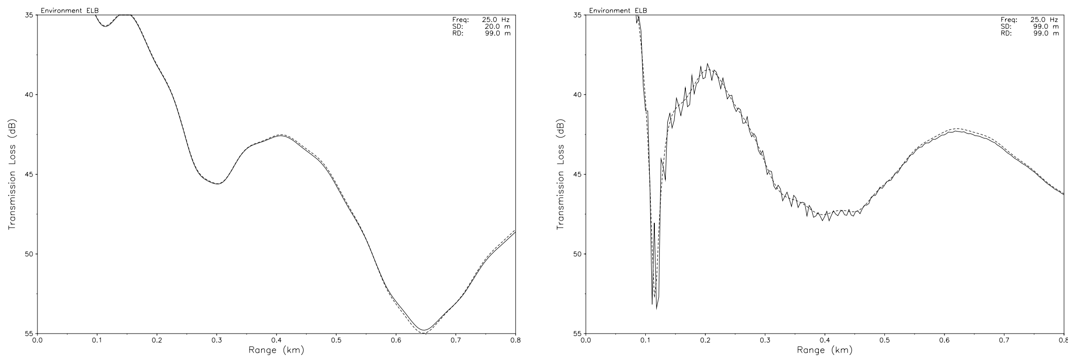

Figure 11: Propagation loss vs range for a receiver at 99 m for source depths of 20 m (left) and 99 m (right). The solid line is for the environment ELB. The dashed line is the propagation loss expected in an environment similar to EL but without shear in the sediment and bottom.

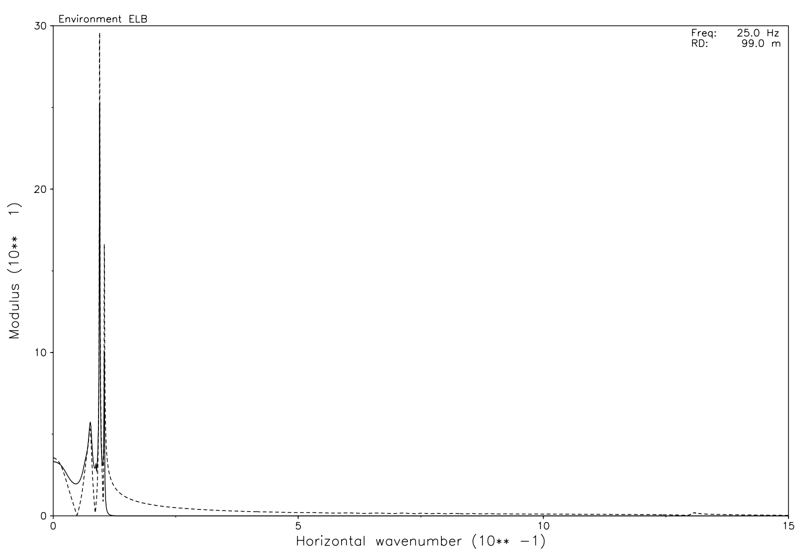

Figure 12: Case ELB: Integrand plots for a receiver at a depth of 99 m at a source frequency of 25 Hz. The source depths are 20 m (solid line) and 99 m (dotted line).

Parameter		True Value	Estimated Mean	nor. sd.
Sediment Thickness	(m)	75.5999	75.7	0.001
Sediment P-wave Speed	(m/s)	1697.81	1698.0	0.0005
Sediment S-wave Speed	(m/s)	134.347	117	0.09
Sediment layer Density	(g/cm^3)	1.88254	1.872	0.05
Basement P-wave Speed	(m/s)	1839.85	1837.0	0.001
Basement S-wave Speed	(m/s)	214.316	218	0.03
Basement layer Density	(g/cm^3)	2.14580	2.170	0.05
Fitness			8×10^{-5}	

Table 2: Case ELB: Inversion results for the various properties.

5. Discussion and Conclusion

The complexities of problems in MFP can be simplified by a careful study of the physical principles of interaction that underly the propagation of acoustic wave-fields in a given environment. In Sec. 3.2, we have shown that the frequency of the acoustic wave-field determines the interaction of the wave-field with various components of the environment, for example, high frequencies are greatly influenced by the surficial sediment properties. The properties of the basement on the other hand have negligible impact on the propagation of high frequencies in an environment where the sediment thickness is more than a few meters. This information was incorporated into the iterative-subspace inversion strategy in which data were selected based on the frequency, to deduce the relevant parameters. This reduced the dimensionality of the search space in each iteration due to the fewer parameters to be estimated at each stage. The algorithms were able to focus on the solution without getting trapped in the local minima which tends to increase in general with the the number of unknown parameters.

One disadvantage of the subspace method is that by restricting the parameter combinations, it might be more difficult to find the global solution. But when the subspaces are found based on physical principles, this is not expected to be the case.

For a wave-field of fixed frequency, the different properties of a given component of the environment have varying degree of influence on the propagation of the wave-fields. As mentioned in Sec. 4.1, the sediment density has less impact on the acoustic wave-field than the sediment sound speed. Therefore we expect the sediment density to be less precisely estimated as compared to the sound speed.

The geometry of measurement of the observed data influences the relative importance of various parameters. For instance, we saw in Sec. 4.2 that the depth of the source determines the extent to which the shear waves are excited in the sediment and bottom. Even if an environment supports the propagation of shear waves, we may not be able to generate shear waves of sufficient intensity to affect the overall sound propagation if the source is too far away from the water-sediment interface. These considerations should be factored into the inversion as they affects the computational time required for the inversion.

References

1. M. D. Collins and W. A. Kuperman, “Focalization: Environmental focusing and source localization,” J. Acoust. Soc. Am. **90**, 1410–1422 (1991).
2. C.E. Lindsay and N.R. Chapman, “Matched field inversion for geoacoustic model parameters using adaptive simulated annealing,” IEEE Oceanic Eng. **18**, 224–231 (1993).

Parameter	SDB True Value	SDB Estimated Mean	SDB Estimated nor. sd.	SDC True Value	SDC Estimated Mean	SDC Estimated nor. sd.
Sediment Thickness (m)	38.0407	37.4	0.02	30.6873	31.4	0.002
Sediment Speed, top (m/s)	1599.33	1585.8	0.02	1530.44	1526.3	0.015
Sediment Speed, bot (m/s)	1658.46	1663.4	0.015	1604.15	1613.9	0.006
Sediment layer Density (g/cm^3)	1.64407	1.807	0.03	1.50088	1.509	0.03
Basement layer Speed (m/s)	1707.46	1705.5	0.010	1689.00	1687.2	0.007
Basement layer Density (g/cm^3)	1.86593	1.98	0.05	1.70064	1.64	0.08
Fitness	3×10^{-3}			6×10^{-4}		

Table 3: Case SD: Inversion results for realizations B and C using global inversion. Case SDA is repoted in Table 1.

Parameter	WAA True Value	WAA Estimated Mean	WAA Estimated nor. sd.	WAC True Value	WAC Estimated Mean	WAC Estimated nor. sd.
Water Depth (m)	115.334	115.3	0.05	119.879	119.3	0.010
Sediment Thickness (m)	27.0790	27.1	0.010	28.9532	29.9	0.020
Sediment Speed, top (m/s)	1516.20	1515.3	0.06	1565.69	1566.1	0.03
Sediment Speed, bot (m/s)	1573.15	1575.1	0.05	1591.76	1594.3	0.04
Sediment layer Density(g/cm^3)	1.53791	1.545	0.02	1.67889	1.691	0.03
Basement layer Speed (m/s)	1751.26	1749.7	0.005	1707.12	1710.5	0.004
Basement layer Density (g/cm^3)	1.85175	1.934	0.16	1.88435	1.850	0.13
Source Range (m)	1220	1220.5	0.04	1290	1275.8	0.015
Source Depth (m)	26.4200	26.22	0.015	28.2302	28.0	0.007
Fitness	1×10^{-4}			3×10^{-4}		

Table 4: Case WA: Inversion results for realizations A and C using iterative-subspace inversion. Case WAB has been analysed in Sec. 4.1.

Parameter	ELA True Value	ELA Estimated Mean	ELA Estimated nor. sd.	ELC True Value	ELC Estimated Mean	ELC Estimated nor. sd.
Sediment Thickness (m)	55.1365	55.0	0.013	34.8417	35.9	0.003
Sediment P-wave Speed (m/s)	1669.35	1669.8	0.005	1674.78	1677.6	0.005
Sediment S-wave Speed (m/s)	130.630	155.7	0.13	180.148	273.2	0.07
Sediment layer Density (g/cm^3)	1.85324	1.867	0.09	1.83790	1.951	0.06
Basement P-wave Speed (m/s)	1728.47	1727.4	0.009	1747.80	1748.8	0.002
Basement S-wave Speed (m/s)	406.911	385.7	0.12	438.752	450	0.04
Basement layer Density (g/cm^3)	2.06771	2.064	0.3	2.05498	2.126	0.16
Fitness	1×10^{-4}			5×10^{-5}		

Table 5: Case EL: Inversion results for realizations A and C using global inversion. Case ELB is repoted in Table 2.

3. P. Gerstoft, “Inversion of seismo–acoustic data using genetic algorithms and *a posteriori* probability distributions,” J. Acoust. Soc. Am. **95**, 770–782 (1994).
4. D.F. Gingras and P. Gerstoft, “Inversion for geometric and geoacoustic parameters in shallow water: Experimental results,” J. Acoust. Soc. Am. **97**, 3589–3598 (1995).
5. A. Tolstoy, “Some thoughts on shallow water environmental inversion problems,” International Conference on Shallow Water acoustics, Beijing, China (1997).
6. C. Siedenburg, N. Lehtomaki, J. Arvelo, K. Rao and H. Schmidt, “Iterative full-field inversion using simulated annealing,” Full Field Inversion Methods in Ocean and Seismo-Acoustics, Kluwer Academic Publishers, Dordrecht, The Netherlands, 121–126 (1995).
7. P. Gerstoft,“SAGA Users guide 2.0, an inversion sofware package,” SACLANT Undersea Research Centre, SM–333, La Spezia, Italy (1997).
8. H. Schmidt, “SAFARI: Seismo-acoustic fast field algorithm for range independent environments. User’s guide,” SR-113, (SACLANT Undersea Research Centre, La Spezia, Italy, 1987).
9. H. Schmidt, “OASES Version 2.0 Application and Upgrade Notes,” Dept. of Oceanic Eng. MIT, (1996).
10. B.L.N. Kennett, M.S. Sambrigde and P.R. Williamson “Subspace methods for large inverse problems with multiple parameter classes” Geophysical Journal **94** 237–247 (1988).
11. D.W. Oldenburg, P.R. McGillivray and R.G. Ellis “Generalized subspace methods for large scale inverse problems” Geophys J.Int **114** 12-20 (1993).
12. P. Gerstoft and C.F. Mecklenbrauker, “Ocean acoustic inversion with estimation of a posteriori probability distributions”, submitted to J. Acoust. Soc. Am. (May 1997).
13. P. Gerstoft, “Global Inversion by genetic algorithms for both source position and environmental parameters,” J. of Computational Acoustics **2**, 251–266 (1994).
14. A. Tolstoy and R. Chapman, “The matched-field processing benchmark problems,” Journal of Computational Acoustics, this issue (1998).
15. F.B. Jensen and M.C. Ferla, “SNAP: The SACLANTCEN normal-mode acoustic propagation model” SM-121, SACLANT Undersea Research Centre, La Spezia, Italy (1979).
16. E. K. Westwood, C. T. Tindle and N. R. Chapman, ”A normal mode model for acousto-elastic ocean environments,” J. Acoust. Soc. Am. **100** (6), pp. 3631-3645, (1996).
17. M. Siderius, P. Gerstoft and P. Nielsen, “Broadband acoustic inversion using a sparse array,” Journal of Computational Acoustics, this issue (1998).
18. C. T. Tindle and Z. Y. Zhang, ”An equivalent fluid approximation for a low shear speed ocean bottom,” J. Acoust. Soc. Am. **91** (6), pp. 3248-3256, (1992).